Technologies and Materials for Renewable Energy, Environment & Sustainability

Aero-Acoustic Description Under Different Temperature Conditions in a Jet Impinging on a Slotted Plate

AIPCP25-CF-TMREES2025-00043 | Article

Aero-Acoustic Description Under Different Temperature Conditions in a Jet Impinging on a Slotted Plate

Bilal EL Zohbi[1, b)], Michel Matar [2, c)], Kamel Abed-Meraim[3, d)], Hassan Assoum[1,3, a)] and Anas Sakout [3, e)]

[1] *Lebanese International University, Mechanical Engineering Department, Lebanon.*
[2] *Beirut Arab University, Mechanical Engineering Department, Lebanon.*
[3] *LASIE UMR CNRS 7356, La Rochelle University, La Rochelle, France.*

[a)] *Corresponding author: h.assoum@bau.edu.lb*
[b)] *bilal.zohbi@outlook.com*
[c)] *m.matar@bau.edu.lb*
[d)] *kabedmer@univ-lr.fr*
[e)] *asakout@univ-lr.fr*

Abstract. In this investigation, the influence of the plate temperature on both aeroacoustics and flow characteristics of a jet impinging from a rectangular nozzle and Re = 3750 was considered. Experiments were conducted using Particle Image Velocimetry Technique (PIV), Infrared Thermography and microphones to simultaneously capture different flow structures, heat transfer behaviour and sound pressure levels. As the plate was heated, the sound pressure level increased by approximately 7 dB, accompanied by the emergence of a secondary frequency peak at 105 Hz. This frequency was linked to the changes that occurred in the vortex convection velocity near the heated plate wall, suggesting a strong coupling between thermal effects and flow instabilities. When the plate was cooled to steady-state conditions, the secondary peak in the frequency spectrum disappeared and the sound pressure level decreased. These findings confirmed the reversible thermal influence on the jet's aeroacoustics response.
Keywords: Heat Transfer, Aeroacoustics, Impinging jets, Rectangular jet, PIV, Infrared measurements.

INTRODUCTION

Many industrial applications such as turbine blades cooling, thermal management of electronic component and material drying depends on impinging jets, making it very crucial for such applications [1]. Beside their heat transfer efficiency, such applications are often accompanied by discomfort as a fact of the acoustic emissions generated due to strong structure interactions, mainly known as self-sustained tones [2].

Extensive studies were conducted to investigate the aeroacoustic mechanisms of impinging jets [3–11], from early analytical studies of edge tones [12] to recent experimental and numerical investigations of rectangular impinging jets on slotted plate [13]. These studies have highlighted the significant role played by large coherent structures and feedback loops in the production of tonal noise. In previous studies exploring the acoustic behaviour of jet impinging on a slotted plate, it was found a strong dependence of the sound pressure levels on Reynolds number and impact distance [14–22]. Later [23–25] expanded the previous findings using Particle Image Velocimetry (PIV) and acoustic correlation analysis, showing complex interactions between pressure signals and velocity fluctuations near the impingement region.

Even though the acoustic characteristics of impinging jets have been extensively studied, the relationship between thermal conditions and flow dynamics remain less understood. Few investigations were conducted to explore how heating/cooling the jet or the surface of impingement can influence the acoustic field. [26] in his investigation showed that the variation of jet's temperature can alter both the sound intensity and the dominant frequency components. On the other hand, [21] have indicated that changing the temperature of the plate resulted in changes in sound pressure levels. [27] extended the previous work and indicated in his investigation that heating the plate resulted in increasing the sound pressure levels in addition to the emergence of new frequency peak in the acoustic spectrum.

In this paper, the authors examined experimentally the influence of the plate temperature on the aeroacoustic response of a jet impinging on a slotted plate from a rectangular nozzle. The experiments were conducted for Re = 3750, using Particle Image Velocimetry Technique, Infrared Thermography, and Microphones to capture the flow dynamics, plate temperature distribution, and sound pressure levels, respectively. Particular attention was given to identify the appearance of new frequency peak and its relation to vortex convection velocity under different plate temperature conditions.

EXPERIMENTAL APPARATUS AND PROCEDURE

Jet Flow Facility and Flow Control

The experimental setup (FIGURE 1) consists of a confined planar jet issued from a convergent nozzle impinging on a slotted aluminium plate. Air is supplied by a compressor located in an isolated chamber and controlled through a frequency chopper to regulate motor power and jet velocity. The maximum exit velocity at the nozzle outlet is 33 m/s (Mach ≈ 0.1). The Reynolds number, $Re = \frac{V_0 \times H}{u}$, is based on the jet's exit velocity V_0, the nozzle height H=10mm, and the kinematic viscosity u. The airflow passes through a 1 m³ damping volume containing three metal grids, followed by a rectangular tube (1250 mm × 190 mm × 90 mm) and a convergent section that forms the jet. The jet impinges perpendicularly on a 250 mm × 250 mm, 4 mm-thick aluminium plate containing a 45° slotted opening matched to the nozzle exit. Room temperature was maintained between 18–20 °C to ensure stable. Reynolds numbers by drawing air from an adjacent temperature-controlled room.

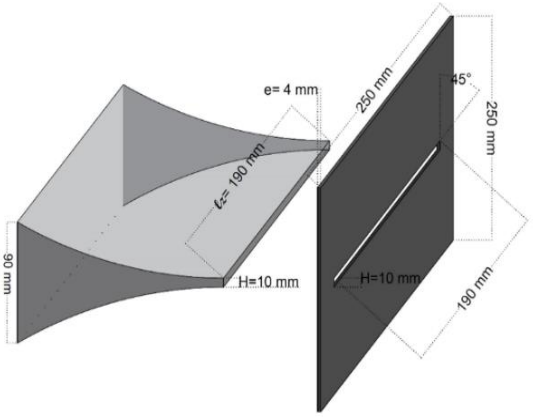

FIGURE 1. Nozzle and slotted plate geometries.

Time Resolved Particle Image Velocimetry (PIV) Measurements

Flow measurements were obtained using a time-resolved PIV system equipped with a Phantom V711 camera (1200 × 800 pixels²) and a 527 nm, 30 mJ laser operated at 1 kHz. The laser sheet was delivered via a mirror arm and converted to a planar sheet using a sheet generator. Olive-oil tracer particles (0.1–0.2 μm) were generated by a LaVision particle generator. The acquisition frequency was 7500 Hz, allowing the capture of coherent flow structures. Synchronization between the laser and camera was achieved through a LaVision High-Speed Controller (HSC). Image pre- and post-processing were performed in DaVis 10.2.1 using 32 × 32 pixel windows with 75% overlap. Vectors with a peak ratio < 1.5 were filtered, and missing data were interpolated bilinearly. The average particle image size was 2.5 × 2.5 pixels, minimizing peak-locking effects. The total measurement uncertainty was estimated at about 2%.

Heat Transfer Measurements

Thermal measurements were obtained using two Xenics Gobi-640-GigE infrared cameras (640 × 480 pixels, 8–14 μm spectral range, 0.05 °C thermal resolution) positioned to capture the upper and lower sides of the slotted plate.

The system provides a spatial resolution of 0.5 mm per pixel in both Y and Z directions. Image acquisition was performed at 50 Hz using Xeneth software for calibration and real-time control. The slotted plate was uniformly heated using self-adhesive Omega-Lux SRMU020409-P heating strips (2.5 W/in², 90 W max each), installed behind the plate. Four FHF05 heat-flux sensors were mounted on the plate to measure local convective fluxes. These sensors, based on thermopile and thermocouple technologies, operate from –70 °C to 120 °C and were fitted with GLD reflective stickers to eliminate radiative effects. The plate was powered by an Asterion AC/DC supply, with voltage adjusted to control surface temperature. Tests were conducted at two target plate temperatures (T1 and T2). During experiments, the plate was continuously heated while being cooled by the impinging jet until a steady-state temperature (TSS) was reached.

RESULTS

FIGURE 2 shows the variation of sound pressure level (SPL) with plate temperature at Re = 3750. As the plate temperature rises to T1 = 60 °C, the SPL increases by about 7 dB. When the plate is cooled by the impinging jet to its steady state (T1SS = 46 °C), the SPL decreases again. Thus, heating the plate enhances the SPL, while cooling reduces it at this Reynolds number.

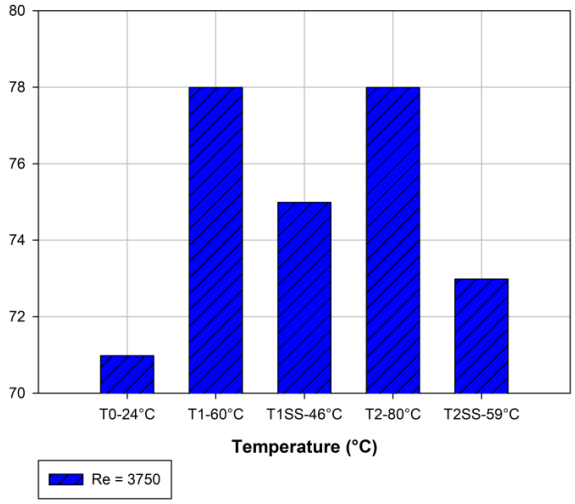

FIGURE 2. Variation of Sound Pressure Levels with plate temperature for Re = 3750.

FIGURE 3 shows the acoustic spectra at different plate temperatures for Re = 3750. As the plate is heated, the SPL and acoustic pressure amplitude both increase. When the plate is cooled under steady-state conditions, the SPL and amplitude decrease again. Notably, a new frequency peak appears at F = 105 Hz during heating and disappears once the plate is cooled.

In order to investigate for the appearance of the sub-harmonic frequency F_2 = 105 Hz when the plate is heated, the transversal velocity spectrum was extracted at four different locations (denoted by points P1 to P4 as shown by FIGURE 4) at all studied temperatures. FIGURE 5-FIGURE 9 show the transversal velocity spectra at four locations for cases T0, T1, T1SS, T2, and T2SS. At ambient conditions (T = T0), both the acoustic and velocity spectra exhibit a dominant frequency at F = 210 Hz across all locations. When the plate is heated (T1 and T2), the acoustic spectrum reveals two peaks at F_1 = 210 Hz and F_2 = 105 Hz. The transversal velocity at points P1 and P2 shows only the 210 Hz component, associated with the Kelvin–Helmholtz vortices in the jet shear layer. In contrast, at points P3 and P4—closer to the heated wall—both frequency peaks (105 Hz and 210 Hz) appear, indicating their contribution to the overall sound pressure level (SPL). When the plate is cooled (T1SS and T2SS), only the 210 Hz peak remains prominent in both acoustic and velocity spectra, while the 105 Hz component becomes barely noticeable at P3 and P4.

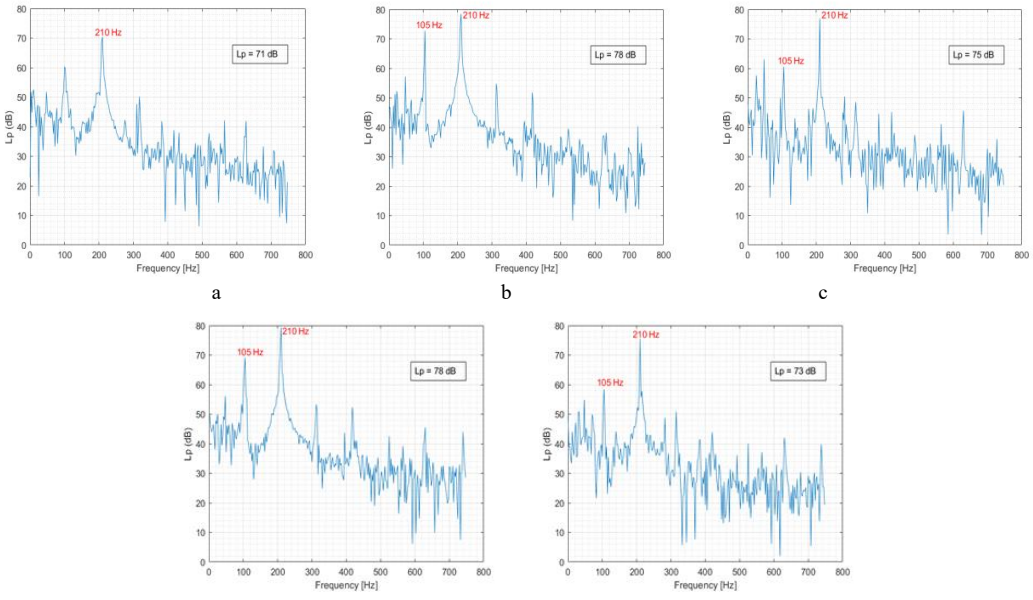

a b c

d e

FIGURE 3a,b,c,d,e. Acoustic spectrum for Re = 3750 at T0, T1, T1SS, T2, and T2SS, respectively.

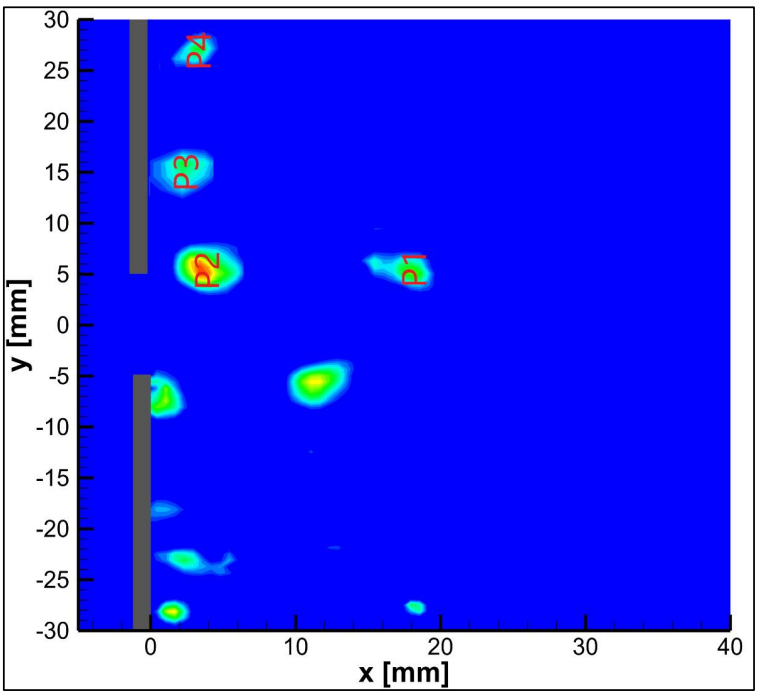

FIGURE 4. λ_2-criterion field showing points at which transversal velocity spectrums are extracted at Re = 3750.

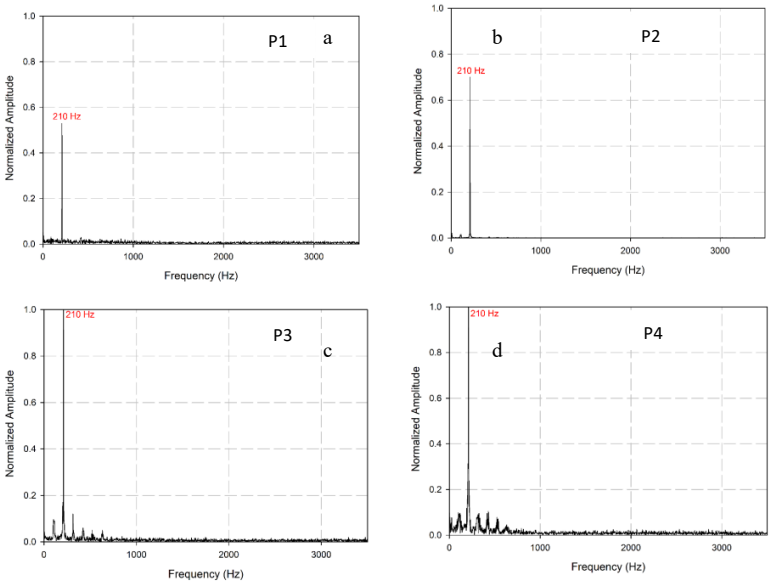

FIGURE 5a,b,c,d. Normalized transverse velocity spectrum for Re = 3750 at T0 extracted at points P1, P2, P3, and P4, respectively.

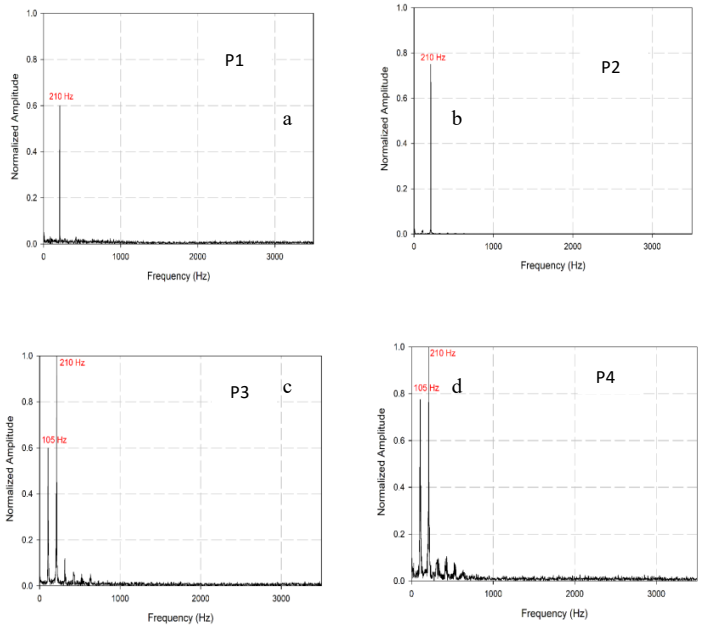

FIGURE 6a,b,c,d. Normalized transverse velocity spectrum for Re = 3750 at T1 extracted at points P1, P2, P3, and P4, respectively.

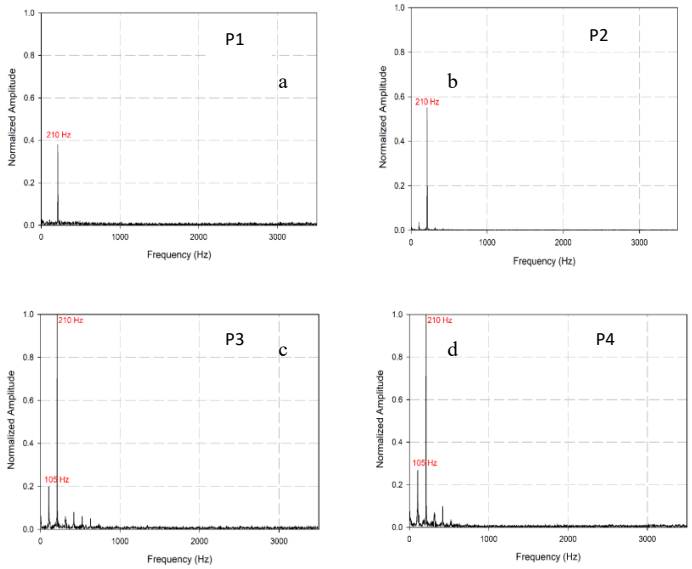

FIGURE 7 a,b,c,d.. Normalized transverse velocity spectrum for Re = 3750 at T1SS extracted at points P1, P2, P3, and P4, respectively.

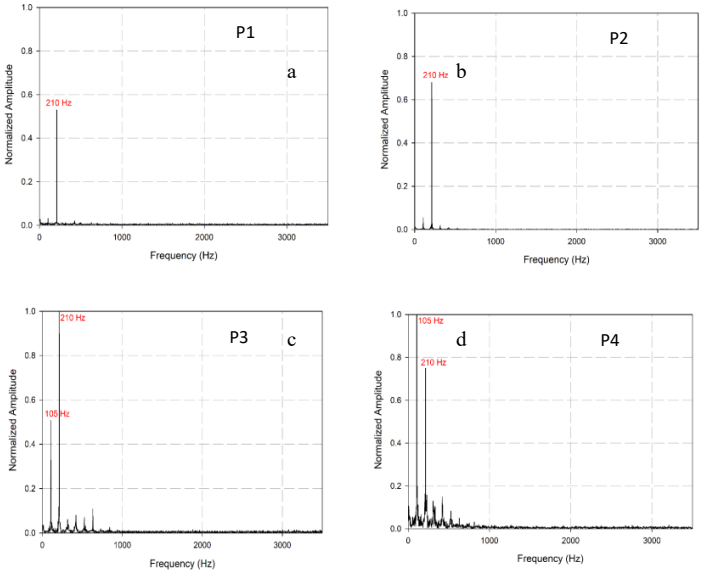

FIGURE 8 a,b,c,d.. Normalized transverse velocity spectrum for Re = 3750 at T2 extracted at points P1, P2, P3, and P4, respectively.

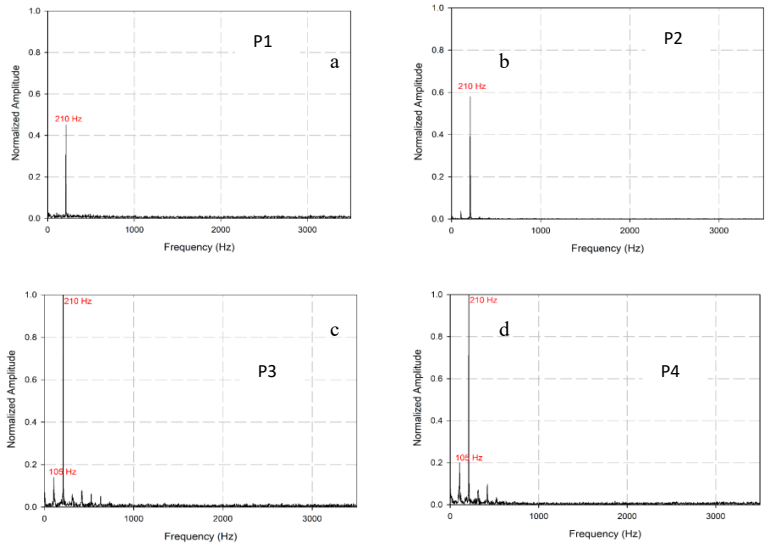

FIGURE 9 a,b,c,d.. Normalized transverse velocity spectrum for Re = 3750 at T2SS extracted at points P1, P2, P3, and P4, respectively.

The vortex convection velocity between points P2 and P3 is estimated in order to see how different temperature conditions affected flow dynamics leading to changes in acoustic spectrum and leading to appearance of frequency F_2 = 105 Hz. Results are shown in TABLE 1. one can notice that when plate is heated to T = T1 and T = T2, the vortex convection velocity increases, when the plate is cooled to T = T1SS and T = T2SS, the vortex convection velocity decreases. Also, one can realize that the lowest convection velocity reached by the vortex between points P2 and P3 is when there was no heating at T = T0.

TABLE 1. showing the vortex convection velocity at different temperature conditions.

Temperature	Convection Velocity
T = T0 = 24 °C	2.46 m/s
T = T1 = 60 °C	2.86 m/s
T = T1SS = 46 °C	2.67 m/s
T = T2 = 80 °C	2.96 m/s
T = T2SS = 59 °C	2.58 m/s

CONCLUSION

Results showed that heating the plate surface altered both the flow dynamics and the acoustic field of the rectangular impinging jet. Elevated plate temperatures enhanced vortex convection and introduced a new frequency at F = 105 Hz, which contributed to higher sound pressure levels at Re = 3750. Conversely, when the plated was cooled, it restored the flow to its original stated and supressed the newly emerged frequency. These findings highlight the sensitive interaction between both aeroacoustics behaviour and thermal changes, offering valuable insight for controlling noise and managing thermal effects in impinging jet applications.

ACKNOWLEDGMENTS

The authors wish to thank FEDER, the ‘Region of Nouvelle Aquitaine’ for the financial support of this research.

REFERENCES

1. El Zohbi, Bilal. *et al.* A Review on Aero-Acoustics and Heat Transfer in Impinging Jets. *International Journal of Technology* **15**, 1398–1419 (2024).
2. Nosseir, N. S. & Ho, C. M. Dynamics of an impinging jet. Part 2. The noise generation. *Journal of Fluid Mechanics* **116**, 379–391 (1982).
3. Choi, J. J., Annaswamy, A. M., Lou, H. & Alvi, F. S. Active control of supersonic impingement tones using steady and pulsed microjets. *Exp Fluids* **41**, 841–855 (2006).
4. Holger, D. K., Wilson, T. A. & Beavers, G. S. Fluid mechanics of the edge tone. *Journal of the Acoustical Society of America* **62**, 1116–1128 (1977).
5. Guerin, S., Allery, C. & Sakout, A. Hysteresis and reduction of self-sustained tones due to a Coanda effect. *Comptes Rendus de l'Académie des Sciences - Series IIB - Mechanics* **329**, 579–584 (2001).
6. Powell, A. On the Edgetone. *The Journal of the Acoustical Society of America* **33**, 395–409 (1961).
7. Chanaud, R. C. & Powell, A. Some experiments concerning the hole and ring tone. *Journal of the Acoustical Society of America* **37**, 902–911 (1965).
8. Hussain, A. K. M. F. Coherent structures and turbulence. *Journal of Fluid Mechanics* **173**, 303–356 (1986).
9. Jeong, J., Hussain, F., Schoppa, W. & Kim, J. Coherent structures near the wall in a turbulent channel flow. *J. Fluid Mech.* **332**, 185–214 (1997).
10. Hussain, A. K. M. F. Coherent structures—reality and myth. *Phys. Fluids* **26**, 2816 (1983).
11. Husain, H. S. & Hussain, F. Experiments on subharmonic resonance in a shear layer. *J. Fluid Mech.* **304**, 343–372 (1995).
12. Brown, G. B. The vortex motion causing edge tones. *Proceedings of the Physical Society* **49**, 493–507 (1937).
13. El Zohbi, B. *et al.* Experimental investigation of the Aero-Acoustics of a rectangular jet impinging a slotted plate for different flow regimes. *Alexandria Engineering Journal* **87**, 404–416 (2024).
14. H. H. Assoum, *et al.* Turbulent Kinetic Energy and Self-Sustaining Tones: Experimental study of a rectangular impinging jet using High Speed 3D Tomographic-PIV. *Journal of Mechanical Engineering & Sciences* (2020).
15. Assoum, H. *et al.* Correlation between the acoustic field and the transverse velocity in a plane impinging jet in the presence of self-sustaining tones. *Energy Procedia* **139**, 391–397 (2017).
16. Assoum, H. *et al.* Spatio-Temporal Changes in the Turbulent Kinetic Energy of a Rectangular Jet Impinging on a Slotted Plate Analyzed with High Speed 3D Tomographic-Particle Image Velocimetry. *IJHT* **37**, 1071–1079 (2019).
17. Assoum, H. H. *et al.* Tomographic Particle Image Velocimetry and Dynamic Mode Decomposition (DMD) in a Rectangular Impinging Jet: Vortex Dynamics and Acoustic Generation. *Fluids* **6**, 429 (2021).
18. El Zohbi, B. *et al.* Experimental investigation of the Aero-Acoustics of a rectangular jet impinging a slotted plate for different flow regimes. *Alexandria Engineering Journal* **87**, 404–416 (2024).
19. Assoum, H. H. *et al.* Control of a rectangular impinging jet: Experimental investigation of the flow dynamics and the acoustic field. *Alexandria Engineering Journal* **79**, 354–365 (2023).
20. Alkheir, M. *et al.* Combined stereoscopic particle image velocimetry measurements in a single plane for an impinging jet around a thin control rod. *Fluids* **6**, 430 (2021).
21. Mrach, T. *et al.* Experimental study of the thermal effect on the acoustic field generated by a jet impinging on a slotted heated plate. *Energy Reports* **6**, 497–501 (2020).
22. Assoum, H. H. *et al.* Energy transfers between aerodynamic and acoustic fields in a rectangular impinging jet. *Energy Rep.* **6**, 812–816 (2020).
23. Assoum, H., Hassan, M. El, Abed-Meraïm, K., Martinuzzi, R. & Sakout, A. Experimental analysis of the aero-acoustic coupling in a plane impinging jet on a slotted plate. *Fluid Dynamics Research* **45**, (2013).
24. Assoum, H. *et al.* Experimental investigation the turbulent kinetic energy and the acoustic field in a rectangular jet impinging a slotted plate. *Energy Procedia* **139**, 398–403 (2017).
25. Assoum, H. H. *et al.* Energy transfers between aerodynamic and acoustic fields in a rectangular impinging jet. in *Energy Reports* vol. 6 812–816 (Elsevier Ltd, 2020).
26. Gustavsson, J., Ragaller, P., Kumar, R. & Alvi, F. Temperature Effect on Acoustics of Supersonic Impinging Jet. in *16th {AIAA}/{CEAS} Aeroacoustics Conference* (American Institute of Aeronautics and Astronautics, Stockholm, Sweden, 2010). doi:10.2514/6.2010-3785.
27. El Zohbi, B. *et al.* Experimental investigation of the Aero-Acoustics of a rectangular jet impinging a slotted plate for different flow regimes. *Alexandria Engineering Journal* **87**, 404–416 (2024).